

Effective Medium Theory, Rough Surfaces, and Moth's Eyes

R. Steven Turley, David Allred, Anthony Willey, Joseph Muhlestein, and Zephne Larsen
Brigham Young University, Provo, Utah

Abstract

Optics in the extreme ultraviolet (XUV) have important applications in microelectronics, microscopy, space physics, and in imaging plasmas. Because of the short wavelengths involved in these applications, it is critical to account for interfacial roughness to accurately predict the reflection and absorption of XUV optics. This paper examines two possible effects of roughness on optical absorption, non-specular reflection and enhanced transmission and compares these to measured experimental data on a rough Y_2O_3 thin film.

Background

The extreme ultraviolet region of the electromagnetic spectrum consists of the wavelengths between about 6×10^{-8} m and 1×10^{-9} m. As you will note in Figure 1, it does not penetrate Earth's atmosphere, has a wavelength between the size of large molecules and atoms, and is the most intensely radiated from objects between about 50,000 K and 3,000,000 K.

This makes these wavelengths ideal for applications such as photolithography, microscopy, astrophysical observations, and plasma diagnostics.

The most reflective mirrors at these wavelengths are made of several layers of thin films of various materials. The best planar mirrors are uniform and smooth at the level of less than 0.5 nanometers. Keeping surface variations to much less than a wavelength justifies the use of approximating the interface as an abrupt change in medium. It also provides the conditions where we would expect the highest specular reflectance from the surface.

Recently, we fabricated a sample we were interested in characterizing which was thicker than we would normally use. The 190 nm film had a roughness of about 3 nm. The attenuation and phase distortion of an extreme ultraviolet wave reflecting from a rough surface scale like

$$\phi = \frac{2\pi d}{\lambda}, \tag{1}$$

where d is the height of the roughness and λ is the wavelength of the light. For this film with our wavelength of 12 nm, ϕ was about 1.

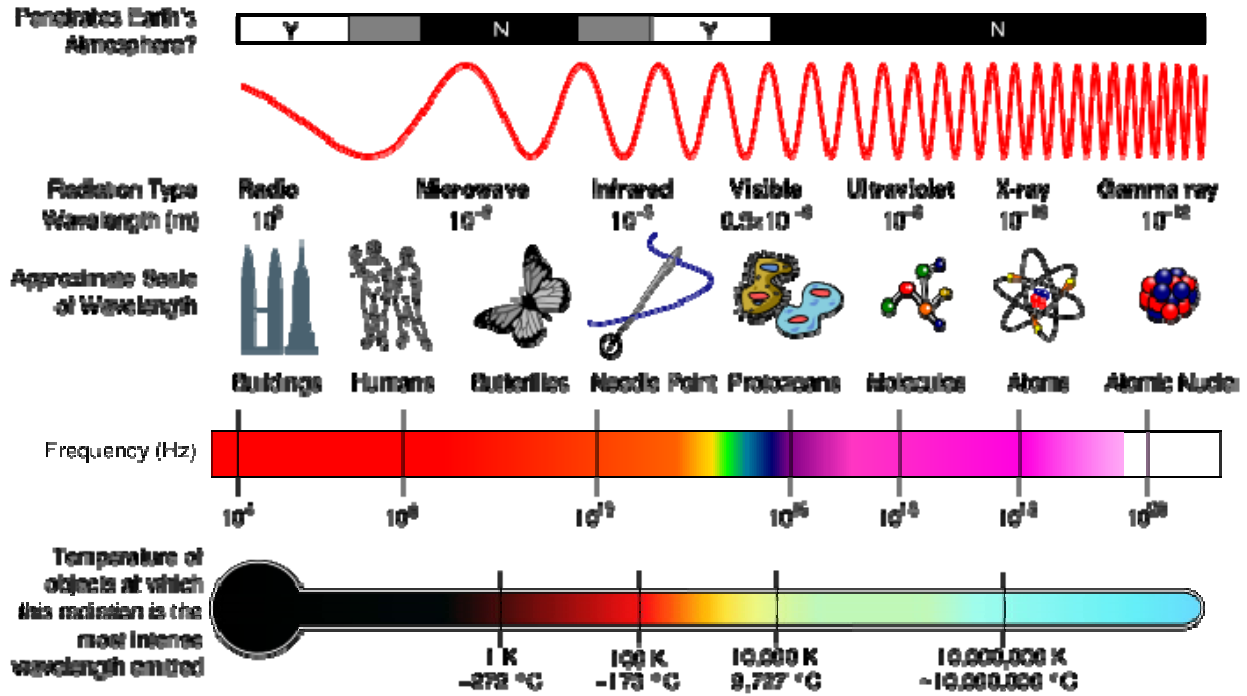


Figure 1: Electromagnetic spectrum.

In order to correctly interpret our data, we needed to be able to correctly account for the effects of this roughness. Depending on the spatial length scale of the roughness we anticipated two possible effects. Depending on the characteristic length scale of the roughness compared to the wavelength of the incident light, the surface could reflect like a projection screen or like a moth's eye. This more qualitative analysis gives us a better feel for interpreting our experimental data than the more rigorous exact computations we have done earlier (Turley, Martin, & Johnson, 2008).

When the characteristic length scale is much larger than the wavelength of the incident light the surface acts like a projection screen or a piece of frosted glass. In this case, the surface scatters light in all directions. Contrast this with reflection in a single direction one would get from a smooth mirror.

When the surface roughness has a depth on the order of a wavelength, but a transverse length scale much smaller than a wavelength it behaves like the moth's eye shown in Figure 2.

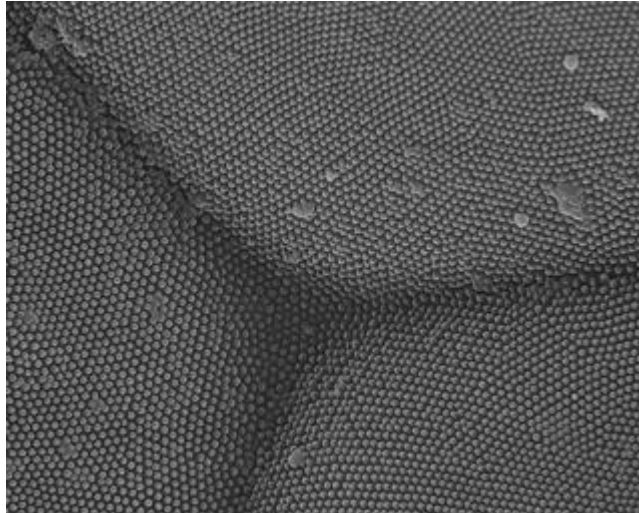


Figure 2: Electron micrograph of a moth's eye.

In a moth, this structure results in a very low reflection from the surface. Instead, the eyes surface transmits light to the moth's cornea very efficiently, making them less visible to predators and giving them better vision in dim light.

Theory

In the limit of surface features which vary over length much longer than a wavelength, the surface can be treated by geometrical optics. At each point of the surface, the angle of the incident beam is compared to the normal to the surface. The reflected light at that point should make the same angle with the normal as the incident light. This idea is illustrated in Figure 3.

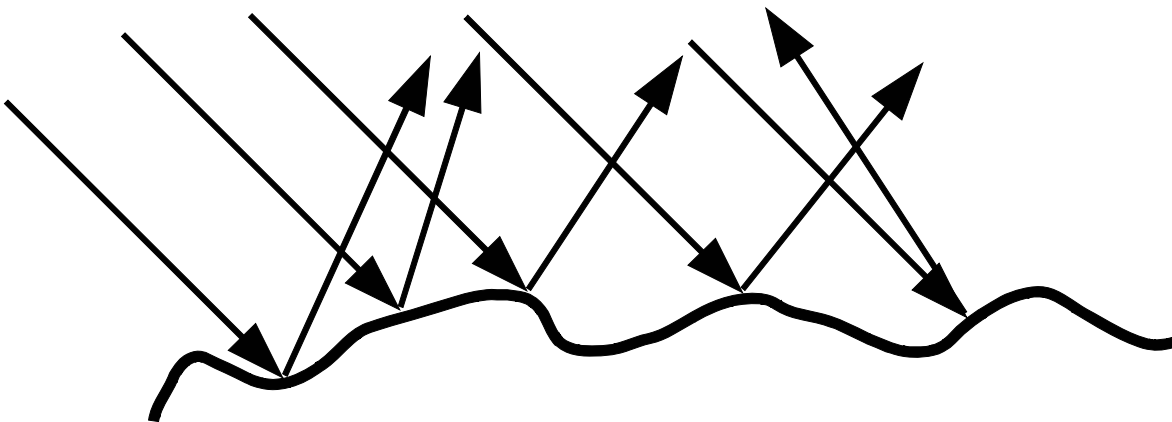


Figure 3: Scattering from a projection screen.

In the case of a surface with lateral variations on a length scale much shorter than the wavelength of the incident light, one can use the average index of refraction over the surface. Thus, the abrupt interface would be replaced with a gradient in the index of refraction as illustrated in Figure 4.

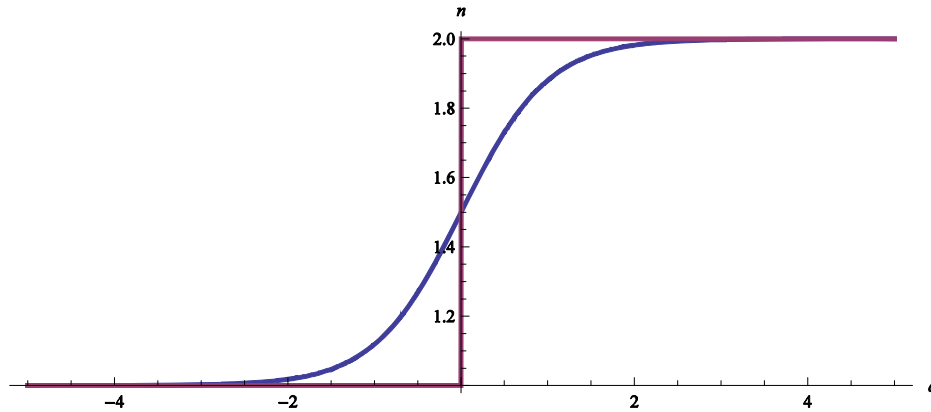


Figure 4: Index gradient representing a rough surface whose lateral variations have a length scale much smaller than the wavelength of incident light. Here n is the index of refraction and d is the distance perpendicular to the surface.

We computed how a beam with a Gaussian spread would be spread out in angle by interacting with a surface using the model illustrated in Figure 3. We considered two surfaces: one with a surface height which varies according to a Gaussian random number and another whose height varies according to a uniform (“linear”) random number. The variations in surface height give rise to a variation in the angle the incident beam makes with the surface at various points. The results are shown in Figure 5. Note that the effects of the roughness are to spread out the beam and decrease the peak height. The linear variation in height produces a flatter scattered beam than the Gaussian surface.

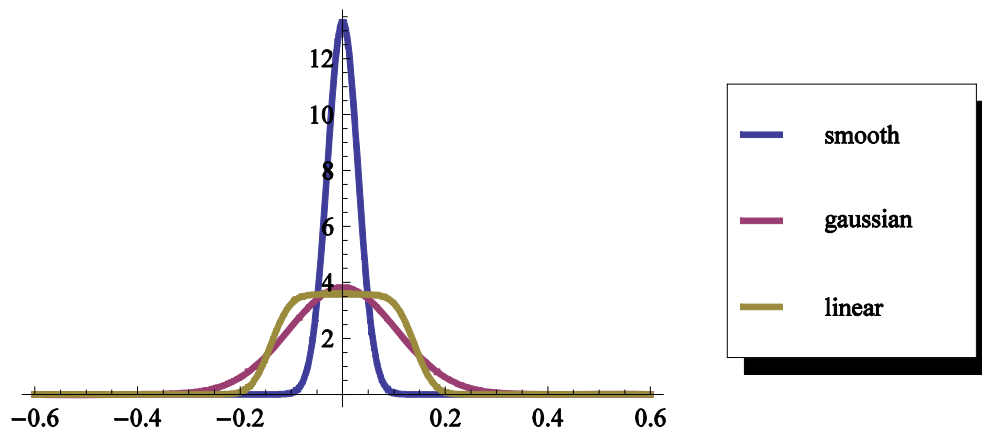


Figure 5: Beam spreading due to a Gaussian and linear roughness of the reflecting surface.

We computed the effects of a gradient in the index of refraction by solving Maxwell’s Equations for a source-free region of space.

$$\nabla \cdot \vec{D} = 0 \quad (2)$$

$$\nabla \cdot \vec{B} = 0 \quad (3)$$

$$\nabla \times \vec{H} = \frac{\partial \vec{D}}{\partial t} \quad (4)$$

$$\nabla \times \vec{E} = -\frac{\partial \vec{B}}{\partial t} \quad (5)$$

We assumed the fields have a time dependence of $e^{-i\omega t}$ and that \vec{D} and \vec{B} are given by relations

$$\vec{D} = n^2(\vec{x}) \epsilon_0 \vec{E} \quad (6)$$

$$\vec{B} = \mu_0 \vec{H} \quad (7)$$

where n is the index of refraction, ϵ_0 is the permittivity of free space, and μ_0 is the magnetic permeability of free space. One can get differential equations for just \vec{E} or \vec{B} by taking the curl of the curl equations, substituting the equations into each other, taking advantage of the curl-curl vector identity, and utilizing the divergence equations. The resulting equation for the electric field is

$$\left(\nabla^2 + [k_0 n(\vec{x})]^2 \right) \vec{E} = 0. \quad (8)$$

We solved this equation for the same two cases considered in short wavelength case. The x direction is taken to be the direction perpendicular to the interface with y and z parallel to the interface. For the one dimensional case of normal incidence and a linear index gradient of width w in the x direction,

$$n(x) = 1 + \frac{n-1}{w} x \text{ for } 0 \leq x \leq w. \quad (9)$$

Substituting Equation (9) into Equation (8) yields

$$\left[\frac{d^2}{dx^2} + k^2 \left(1 + \frac{n-1}{w} x \right)^2 \right] B(x) = 0. \quad (10)$$

This has the solution

$$B(x) = c_2 D_{-\frac{1}{2}}[(n-1)g(x)] + c_1 D_{-\frac{1}{2}}[(1+n)g(x)] \quad (11)$$

where

$$g(x) = \frac{\sqrt{k(w + (n-1)x)}}{\sqrt{(n-1)w}} \quad (12)$$

and the functions D are parabolic cylinder D functions. This solution in Equation (11) was matched with its amplitude and derivative to an incident plane wave of unit amplitude and a reflected wave of amplitude B for $x < 0$ and a transmitted wave of amplitude D for $x > w$. The reflected light is specular (in a single direction), but will decrease with thickness as shown in Figure 6. The reflectance is decreased due to increased transmission, not because the reflected light is scattered in all directions. This transmitted light is then absorbed in the thin film and substrate because of the large imaginary part of the index of refraction typical of materials in the extreme ultraviolet.

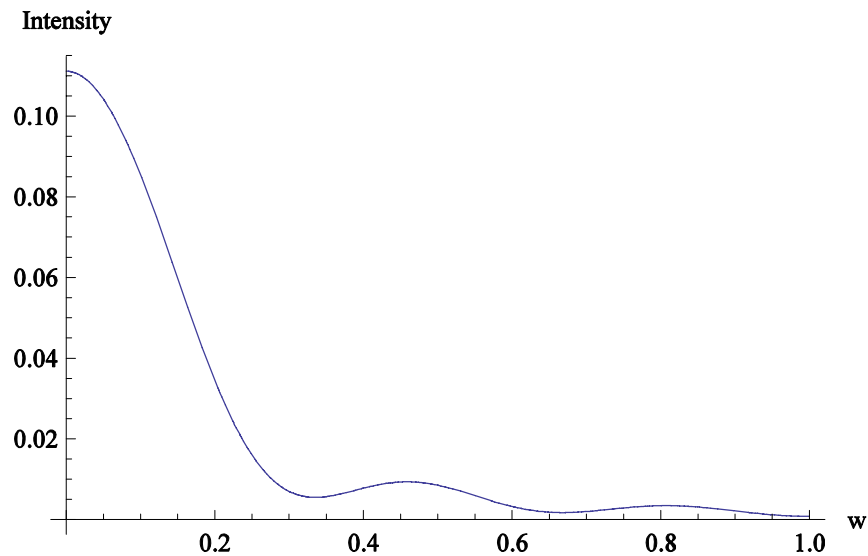


Figure 6: Reflection from an interface with a linear gradient in the index of refraction. The horizontal axis is the width w of the transition layer measured in wavelengths.

The reflection from an interface with a Gaussian roughness cannot be determined analytically. The numerical solution is shown in Figure 7. Details of the numerical calculation are included in the appendix.

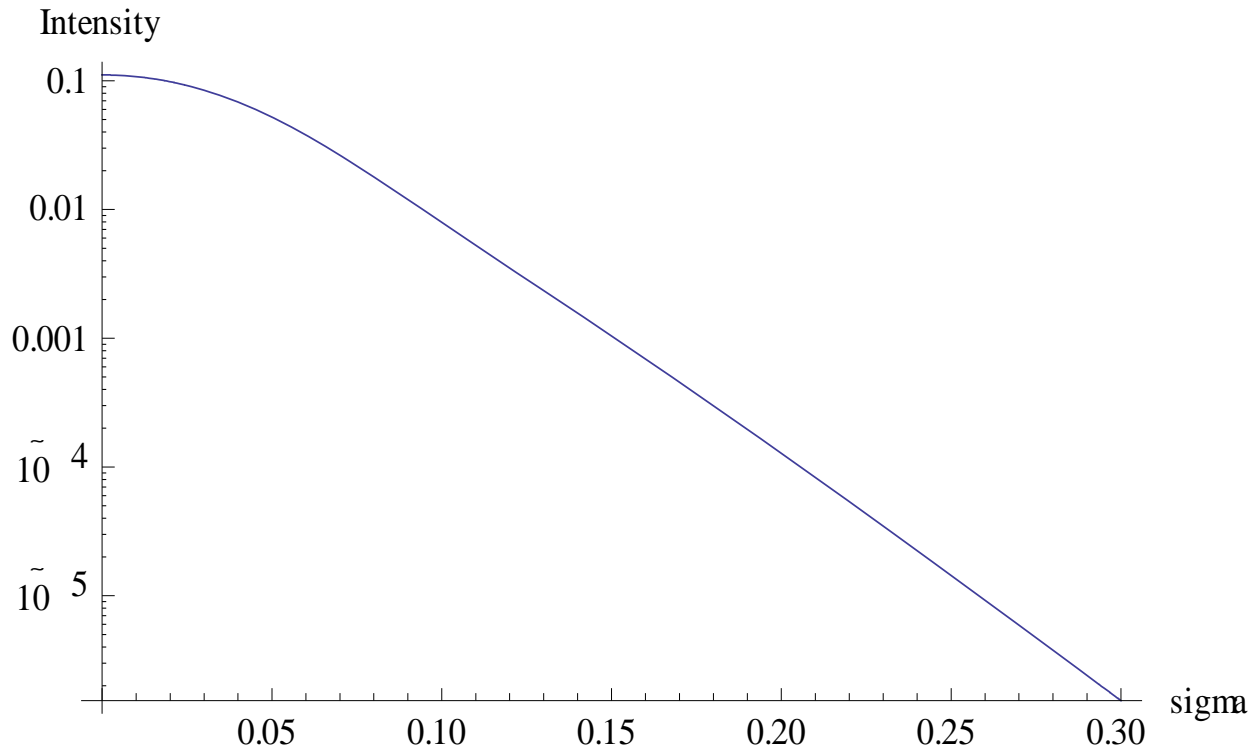


Figure 7: Reflection from a surface with a Gaussian roughness profile. The horizontal axis is the root mean square width of the Gaussian roughness distribution.

Both of these calculations agree well with the commonly used Nevot-Croce (Croce & Nevot, 1976) roughness corrections for small roughness amplitudes. The linear gradient and the Nevot Croce calculations are compared in Figure 8.

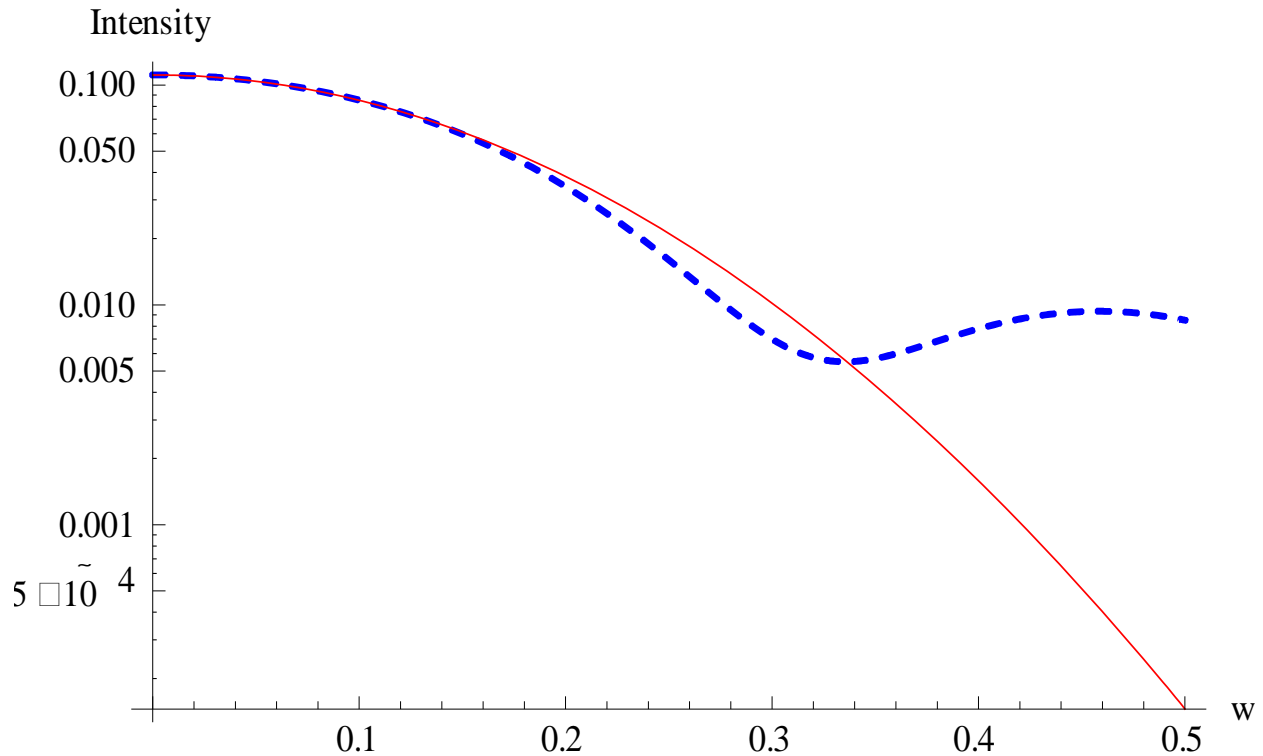


Figure 8: Comparison of linear gradient and Nevot-Croce corrections for surface roughness. The solid red curve is the calculation with a linear gradient. The dotted blue curve is the Nevot-Croce correction with $\sigma = 0.29w$, the rms “roughness” of a layer with a linear gradient.

Comparison with Experiments

To determine which physical picture of scattering from our rough surface was the most suitable, we made two types of measurements using Beamline 6.3.2 of the Advanced Light Source at Lawrence Berkeley National Laboratories. One set of measurements were a direct measure of the reflectance of a thin film of RF-sputtered Y_2O_3 about 200 nm thick. The other was a measure of the width of the reflected beam.

These data were fit to the Parratt formula for reflectance of a stack of thin films as described in Muhlestein’s Honors thesis (Muhlestein, 2009). The measured data were fit to this formula to determine a global thickness of the Y_2O_3 film as well as the complex index of refraction at the various wavelengths. The weight shown in Figures 9 and 10 was used in the fit to give each measured reflectance roughly equal contributions to the overall determination of the index of refraction. Details are in the thesis.

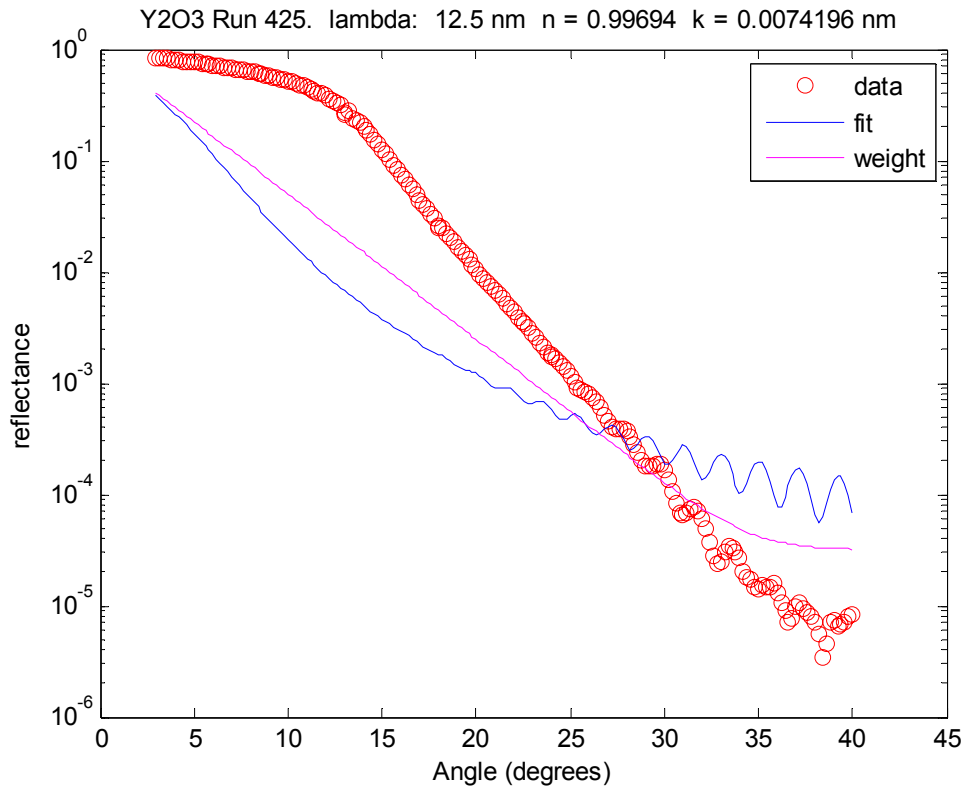


Figure 9: Measured and fit reflectance of our thin film without including a roughness correction. The angles in the figure are measured from grazing.

Figure 9 is a plot of our measured reflectance data compared to a theoretical curve which did not include a correction for surface roughness. The fit reflectance is off by as much as a factor of 100 in some places. It has a qualitatively wrong shape and poor values for the fit index of refraction.

Note the vast improvement in the fit shown in Figure 10. This fit includes a Nevot-Croce correction for surface roughness. We have not yet incorporated the index gradient into our fitting codes, so that direct comparison was not possible.

These fits show the importance of including the effects of surface roughness in our calculations. By themselves, they unfortunately do not distinguish between moth's eye kind of roughness and projection screen kind of roughness.

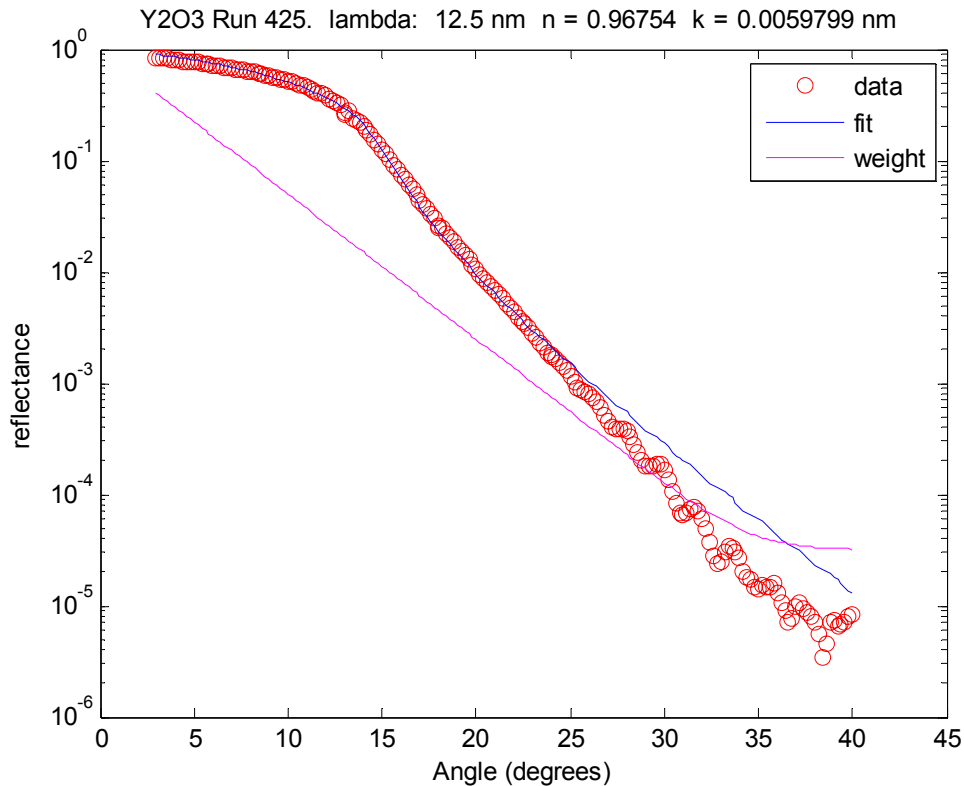


Figure 10: Fit of reflectance data including a Nevot-Croce correction for surface roughness. The angles in the figure are measured from grazing incidence.

We made an additional set of measurements to determine whether the loss of reflectance due to roughness was because of scattering of the reflected light or increased transmission and subsequent absorption. In these measurements, we scanned the detector over a range of reflection angles while keeping the angle of the mirror fixed. These measurements corresponded to the calculations illustrated in Figure 5. If the decreased reflectance was due to scattering, we should have seen an increase in the angular width of the reflected beam. As shown in Figure 11, no such spread in the reflected beam was seen. Thus, it would seem that the reflectance decreased due to increased transmission with subsequent absorption rather than increased scattering.

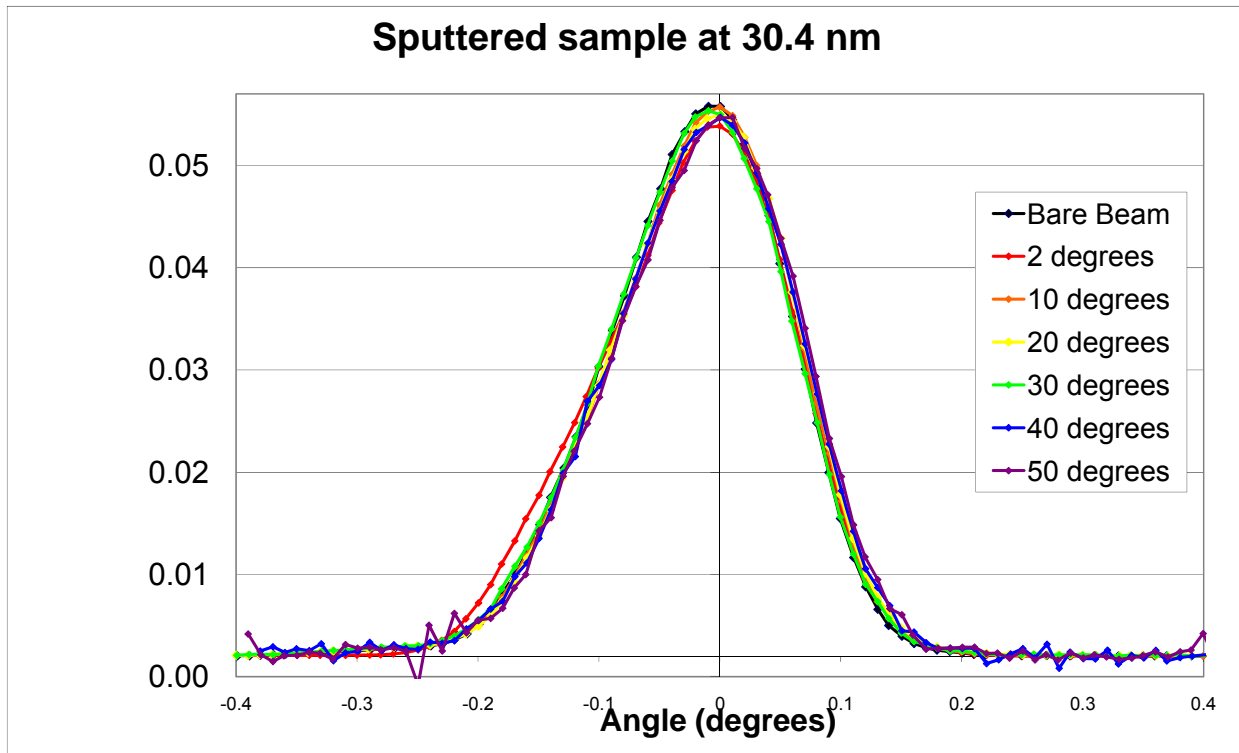


Figure 11: Angular spread of reflected beam at various angles of incidence measured relative to grazing.

Conclusions

The decreased reflectance from our very rough sample seems to have been a result of increased absorption as in a moth's eye surface. Had it been due to increased scattering, we would have expected to see a broadening of the beam. We plan to pursue this question further by measuring the transmission of a similarly rough sample and see if transmission into the film is greater than is the same for a smooth film. We are also planning on altering our data fitting programs to allow modeling of the surface roughness by an index gradient model instead of the current Nevot-Croce model. We also plan on refining our exact numerical codes reported in (Turley, Martin, & Johnson, 2008) to look at the transmission at the interface as well as reflectance.

These results show promise not only for better understanding EUV optics, but also illustrating how these kinds of surfaces could provide more efficient capture of incident light rays in devices such as solar cells as first suggested in (Clapham & Hutley, 1973) and demonstrated in (Sun, Jiang, & Jiang, 2008).

Acknowledgements

The authors are grateful for support received by the National Science Foundation (PHY-0552795), the Department of Energy, and Brigham Young University.

Bibliography

Clapham, P. B., & Hutley, M. C. (1973). *Nature* , 244, 281.

Croce, P., & Nevot, L. (1976). *J. De Physique Appliquee* , 11, 5.

Muhlestein, J. (2009). *Optical Constants for Y2O3 in the Extreme Ultraviolet*. Brigham Young University. Provo, Utah: (<http://www.physics.byu.edu/Thesis/view.aspx?id=203>, accessed 11 March 2010).

Sun, C.-H., Jiang, P., & Jiang, B. (2008). Broadband moth-eye antireflection coatings on silicon. *Appl. Phys. Lett.* , 92.

Turley, R. S., Martin, E., & Johnson, J. (2008). Surface Roughness of Thin Films. *Journal of the Utah Academy of Sciences, Arts, and Letters* , 161--171.

Notes to the Editor

Source of Figures

Figure 1: Wikimedia (public domain)

Figure 2: <http://www.physorg.com/news122899685.html> (credited to Peng Jiang, an Assistant Professor at the University of Florida)

Others: generated by the authors